Analytical Methods

Accepted Manuscript

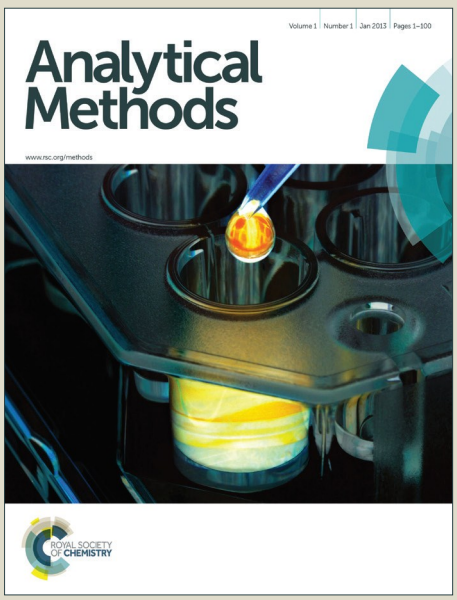

This is an *Accepted Manuscript*, which has been through the Royal Society of Chemistry peer review process and has been accepted for publication.

Accepted Manuscripts are published online shortly after acceptance, before technical editing, formatting and proof reading. Using this free service, authors can make their results available to the community, in citable form, before we publish the edited article. We will replace this *Accepted Manuscript* with the edited and formatted *Advance Article* as soon as it is available.

You can find more information about *Accepted Manuscripts* in the Information for Authors.

Please note that technical editing may introduce minor changes to the text and/or graphics, which may alter content. The journal's standard Terms & Conditions and the Ethical guidelines still apply. In no event shall the Royal Society of Chemistry be held responsible for any errors or omissions in this *Accepted Manuscript* or any consequences arising from the use of any information it contains.

ROYAL SOCIETY OF CHEMISTRY

www.rsc.org/methods

Nanocomposite of ferrocenoyl glutaric acid hydrazone and multiwalled carbon nanotubes as a sensor of azide ion

Ida Tiwari*, Mandakini Gupta, Abhishek Rai, Lallan Mishra

Centre of Advanced Study, Department of Chemistry, Faculty of Science, Banaras Hindu University, Varanasi (INDIA)-221005.

Abstract:

Nanocomposite containing ferrocenoyl glutaric acid hydrazone and multiwalled carbon nanotubes (MWCNTs) has been synthesized and characterized for its structure, morphological and electrochemical properties. Characterization has been done with scanning electron microscopy (SEM), transmission electron microscopy (TEM), thermogravimetric analysis (TGA), infra red (IR), x-rays photoelectron spectroscopy (XPS), UV-visible studies. Electrochemical behavior and stability of modified electrode has been investigated using cyclic voltammetry (CV) and differential pulse voltammetry (DPV). Self-standing film of this electroactive and homogeneous composite has been obtained by solution casting method.

It is observed that ferrocenoyl glutaric acid hydrazone (L)/MWCNTs/nafion composite has better electrochemistry, electrical properties and firm adhesion of the material at the electrode surface. The modified electrode showed electro-catalytic response to the oxidation of azide ion at the potential of 0.30 V in 0.1 M phosphate buffer solution, pH 7.1. The linear range and detection limit for the azide ion was found to be 0.02 mM to 20 mM and 0.312 μM respectively.

Keywords: Modified electrode; multiwalled carbon nanotubes**;** ferrocenoylhydrazone; nanocomposite; azide; sensor

* **Corresponding authors:**

Ida Tiwari:Tel: +91-542-6702444; Fax: +91-542236817;Email:*idatiwari@bhu.ac.in*

1. Introduction:

Azides are reactive chemicals, highly toxic and present health hazard at relatively modest levels in the forms of headache, cytochrome oxidase inhibition and vasodilation.[1] The toxicity is often compared with that of cyanide salts as they give similar symptoms. On the other hand, it is readily protonated in the aqueous environment to yield volatile hydrazoic acid that can create airborne hazard.[2] Small quantities of this highly toxic substance are used in the preparation of biocides, explosives detonators, laboratory preservatives, as a radical scavenger, in the formulation of gas absorbing material in electric discharge tubes, in anticorrosion solutions and to inflate airline safety chutes.[3-4] Because of industrial and pharmacological significance of the azide, a sensitive and reliable method is required for its identification in real time.

Several methods have been reported for the determination of azide like chromatographic methods,[5-6] ceric oxidimetry,[1] titration methods[7-8] etc. A micro diffusion extraction combined with a spectrophotometer is also reported.[9] Several azide-selective electrodes based on relatively selective interaction of transition metal complexes with azide ions have also been reported.[10-11] Generally, gas chromatography, ion chromatography, and capillary electrophoresis are used to detect azide anion with quantifiable limits in the high ppb to low-ppm range but there is problem associated with the reproducibility of the results and expensive chemical requirements. In this context, electrochemical method of analysis are found to be cheaper and can provide high sensitivity, long-term response stability, and good assay reproducibility for analytes that are amenable to such detection.[12-14] It is well documented that azide ions are electrochemically active at carbon, platinum and gold electrodes[1,15] but surprisingly, there have been only a few reports on the electrochemistry of this anion probably due to high overpotential required for its oxidation. Hence, to decrease the required overpotential for azide oxidation, it is necessary to modify the electrode surface.

Ferrocene and its derivatives have been used as redox mediator in composite preparations since long time and have found extensive analytical applications in areas like homogeneous catalysis,[16] nonlinear optics[17] and molecular sensors[18-19]etc. The design of ferrocene-based anion receptors is another area of current intense research.[20] Moreover, the ferrocene and its derivatives have also been organized onto electrodes to construct high redox active systems using covalent binding,[21] Langmuir–Blodgett techniques,[22] self-assembled monolayers,[23] screen-printed[24] designs etc in order to construct artificial molecular devices and sensitive disposable biosensor.[25]

These inorganic complexes act as efficient mediators but they leach out from electrode to the bulk solution due to its low molecular weight.[26-27] Hence, their modification with suitable additives is desirable. Carbon nanotubes (CNTs) posses unique properties such as good electrical conductivity, high chemical stability, and extremely high mechanical strength[28] and also found to promote electron transfer reactions when used as electrode material along with mediators.[28-32] The interesting electrocatalytic properties of CNTs are mostly due to the presence of defects like the edge planes of pyrolytic graphite located mainly at the ends of tubes.[29] However, main limitation with their use owes to poor solubility of multiwalled carbon nanotubes (MWCNTs) in water due to their hydrophobic nature. CNTs have been successfully solubilized with nafion for further use.[31] Nafion has been reported as an effective exchanger for different metal complexes, but the rate of electron transfer is very slow in nafion film alone.[26] The porous structure of the nafion provides entry point for analytes and nano-sized hydrophilic pockets can act as accumulation volume[33] and the electron transfer rate of nafion is improved in presence of CNTs. Herein, we have incorporated a synthesized derivative of ferrocene, ferrocenoyl glutaric acid hydrazone (designated as L) with MWCNTs and nafion to increase the electron shuttle. To the best of our knowledge, no reports are available for electrochemical azide sensor using a nanocomposite of ferrocenoyl hydrazone with nafion coated MWCNTs.

This paper embodies the synthesis and characterization of nanocomposite of L with nafion coated MWCNTs together with its application in selective detection of azide anion.

2. Materials and Methods

2.1 Reagents and materials

The solvents purchased from E. Merck were freshly distilled prior to their use. Ferrocencarboxaldehyde, multiwalled carbon nanotubes (diameter 110–170 nm, length 5–9 μm, purity 90+ %); nafion (5% commercial solution) and tetra butyl ammonium azide were purchased from Sigma–Aldrich Chem. Co (USA). Other chemicals were of analytical grade. All solutions were prepared with triple distilled water. All the experiments were performed in 0.1 M phosphate buffer solution (pH 7.1). The stock solution of 0.01 M of L was prepared by dissolving it in 1 ml DMF and then stored in a refrigerator.

2.2 Instruments

CHI 630C series (USA) electrochemical system was used for the electrochemical studies. The three electrodes system was used for the cyclic voltammetry in which nanocomposite modified glassy carbon electrode (GCE) acted as working electrode, Ag/AgCl/3M KCl as reference electrode and Pt wire as counter electrode. All electrochemical measurements were carried out in 10 mL phosphate buffer solution (PBS), pH 7.1 purged with nitrogen for 10 min prior to measurements. The UV–visible spectroscopic measurements of an aqueous solution of L and L/MWCNTs/nafion nanocomposite were carried out using a UV-visible spectrophotometer (Hitachi U-3900, Japan), SEM of nanocomposite film has been done with JEOL840A; Japan. TEM measurements of MWCNTs and L/MWCNTs/nafion nanocomposite were performed on a Tecnai G2 instrument (200 kV). The samples were dispersed in distilled water and deposited onto a formvar/carbon coated copper grid for TEM measurements. IR spectra were recorded using KBr pellets on a Varian 3100 FT-IR in the 4000–400 cm^{-1} region. ^{1}H-NMR spectra of L were recorded in DMSO-d_6 using a JEOL AL 300 FT-NMR spectrometer at room temperature. X-ray photoelectron spectroscopy (XPS) studies were carried out in a VG Microtech Multilab ESCA 3000 spectrometer with a non-monochromatized Al Kα X-ray (hv = 1486.6 eV) and TGA has been performed by Perkin Elmer (STA 6000). Electrospray ionization mass spectrometry (ESI-MS) was carried out on an AMAZONSL Max ion trap mass spectrometer.

2.3 Preparation of ferrocenoyl glutaric acid hydrazone (L):

Ferrocenoyl glutaric acid hydrazone was prepared as shown in Scheme 1 by refluxing an ethanolic solution of ferrocene-4-carboxaldehyde (2.0 mmol) with ethanolic solutions of glutaric acid hydrazide (1.0 mmol) on a water bath for 8–9 h. Corresponding brown solid compound thus obtained was filtered off, then recrystallized from ethanol and dried *in vacuo*. The data related to the synthesis of glutaric acid hydrazide is shown as table 1.

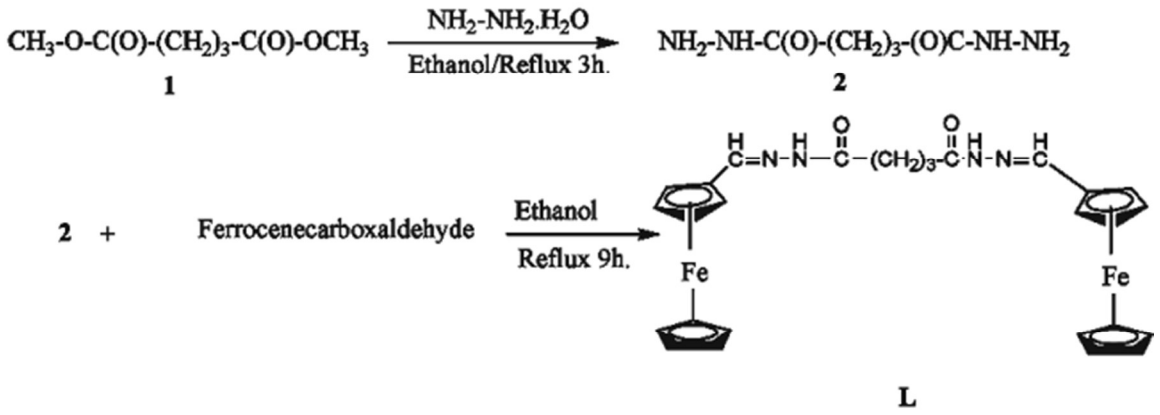

Scheme 1. Synthesis of Ferroceyl hydrazone.

2.4 Preparation of L/MWCNTs/nafion nanocomposite modified electrode:

GCE was polished on polishing kit using 1µ, 0.3µ, 0.05µ particle sized alumina. GCE was washed in acetone, then ultrasonicated in distilled water and allowed to dry at room temperature. The crude MWCNTs were purified and treated to acquire negative charge using method as reported earlier with some modification.[33] Nafion solution (1mL, 1.1 %) was prepared by diluting it with triple distilled water followed by the dispersion of 0.5 mg of purified MWCNTs in 50 µL nafion solution and was then ultrasonicated for half an hour to make a homogenous solution of MWCNTs/nafion. This solution (5 µL) was then drop casted on a cleaned GCE and was allowed to air dry for 1 hour. A solution of L (0.01M, 5 µL) was then dropped over modified MWCNTs/nafion GCE and left at room temperature for drying for 2-3 hours.

3. Results and discussion:

3.1 Physical characterization of ferrocenoyl glutaric acid hydrazone (L):

The compound L was characterized by mass analysis (Fig. S1), ^{1}H NMR (Fig. S2), ^{13}C NMR (Fig. S3) and IR (Fig. S4). The IR spectrum of L indicates ν_{max} (KBr) (cm^{-1}): 3060, 3030 (NH), 1640 (C=O), 1601(CH=N), 812(cp), 507, 482 (Fe-cp). In ^{1}H NMR spectrum, signals observed at δ_{ppm} 11.0, 10.9 marked the presence of -NH protons. However, peaks observed between 4.82-

4.19 ppm were assigned to ferrocene protons. ESI-mass analysis gave peak at 553.0983 corresponding to parent ion peak $[M+H]^+$.

3.2 Physical characterization of L/MWCNTs/nafion nanocomposite:

3.2.1 SEM studies:

A SEM image of MWCNTs together with nafion shown in Fig. 1 (A) indicated a closely woven network of fibres. Hole like appearance can be seen in the image. However, SEM micrograph of nanocomposite L/MWCNTs/nafion shown in Fig. 1 (B) appeared homogeneous with a well dispersed pattern of uniform morphology. The presence of interwoven and interconnected thread like structures can be clearly seen with spots which are likely due to presence of L on modified MWCNTs dispersed in the homogeneous porous nafion matrix which helps in increasing the electron transfer at electrode surface. The hole like appearance disappeared due to the adsorption of L over the nafion/MWCNTs surface. The surface area of nanocomposite increased as compared to Fig. 1 (A) indicating that nafion acts as an efficient matrix for preparation of nanocomposite with high surface to volume ratio.

3.2.2 TEM studies:

Figure 1 (C) shows TEM image of the modified pure MWCNTs with nafion which appeared smooth and clear showing no adsorption. TEM image of nafion/MWCNTs display film like structures which strongly supports that nafion molecules are chemically adsorbed on the MWCNTs and MWCNTs have not been re-aggregated as already reported earlier.[32] It is likely that the hydrophobic chain of nafion interacts with MWCNTs and therefore the MWCNTs are functionalized with negatively charged sulphonic groups resulting in well dispersed MWCNTs.[32] Figure 1 (D) shows the TEM image of L/MWCNTs/nafion nanocomposite. The walls of L/MWCNTs/nafion nanocomposite have some dark spots and appear to be rough in nature. The probable interaction between L and nafion coated MWCNTs are proposed to be strong electrostatic interaction between negatively charged sulphonic groups at the walls of MWCNTs with L. Hence, it can be concluded that MWCNTs are coated with nafion which can adsorb L forming nanocables type structure. The network of nanocables offers more possibilities to enrich the surface chemistry of MWCNTs and of increased sensor response.

3.3 Thermogravimetric analysis (TGA):

TGA scan of pure MWCNTs (curve a), MWCNTs/nafion (curve c), and L/MWCNTs/nafion (curve b) nanocomposite in air atmosphere is illustrated in Fig. 2. It is apparent that the thermal degradation is very different for all the three samples. The temperature corresponding to the onset of thermal degradation (Ton) and the slope of mass loss (%) is different for different composite materials. Fig. 2 shows pristine MWCNTs exhibits excellent thermal behavior and do not show significant weight loss (less than 5 percent) upto the temperature of 600^0 C (curve a)[34-35] after that degradation of C back bone start. The Fig.2 also indicates that the 1st weight loss (%) from 30^0C to 320^0C for L/MWCNTs/nafion (curve b) and MWNTs/nafion (curve c) composite material appeared on account of boundary water loss which could not be completely evaporated at 100^0C. The evaporation temperature of water is higher due to the interaction of sulphonic acid groups of nafion resin. The 2nd weight loss appeared in a range of 320–430^0C due to the desulphonation process and the third degradation stage around 430–530 ^{0}C is associated with the polytetrafluoroethylene backbone degradation.[36-37] It is well reported in literature that nafion is thermally stable upto 250^0 C. [38] This indicates that the incorporation of MWCNTs and L to nafion further increased the thermal stability of the nafion which provides an evidence for the composite formation. The L/MWCNTs/nafion (curve b) TGA scan is intermediate between the pure MWCNTs (curve a) and MWCNTs/nafion (curve c) TGA scan. The thermal degradation range of L/MWCNTs/nafion is less than MWCNTs/nafion which indicates the incorporation of L imparts better thermal stability to prepared nanocomposite as compared to MWCNTs/nafion composite.

3.4 XPS studies:

XPS analysis of pure MWCNTs (*cf.* Fig. 3, curve a) shows peak at 284.3 eV for C. After dispersion of MWCNTs in nafion solution, the chemical structure shows the presence of the nafion chains in MWCNT/nafion as discussed by Ying Ling Lui *et al*.[39] The large fluoride signal and the sulfur signal in the wide scan spectrum of MWCNTs/nafion indicates successful incorporation of nafion chains to MWCNTs (results not shown). After addition of L in MWCNTs/nafion composite (curve b), the spectrum of L/MWCNTs/nafion shows peak components with binding energies at 286.6 eV for the C–O species, at 291.5 eV for the C–F species, at 292.3 eV for the CF_2 species, at 293.0 eV for the CF_3 groups and at 710 eV and 725

eV for the Fe. Wide spectrum of Fe can be seen in the inset I of Fig.3. In the inset II of Fig. 3; C, CF_2 and CF_3 spectrum is clearly visible in wide spectrum of C 1s core-level spectrum of MWCNTs, MWCNT/nafion and L/MWCNTs/nafion composites. The intensity of C-C peak was highest in pure MWCNTs (curve a) with binding energy at 284.3 eV. After dispersion in nafion, C-C peak intensity of MWCNTs/nafion (curve b) decreased with binding energy at 285 eV and finally, incorporation of L resulted in L/MWCNTs/nafion (curve c) composite where C-C peak intensity further decreased and peak shifting occured with binding energy at 283.8 eV. These data suggest successful preparation of L/MWCNTs/nafion nanocomposite.

3.5 UV–visible characterization of L/MWCNTs/nafion nanocomposite:

The prepared L/MWCNTs/nafion composite was characterized by its UV-visible spectrum recorded in DMSO-water solution (1:9) in the range of 300-700 nm as displayed in Fig. 4(c). Its spectrum was compared with the spectra of MWCNTs/nafion (aqueous solution) and of L in DMSO-water solution (1:9) as shown in Fig. 4(a) and Fig. 4(b) respectively. The UV–visible spectrum of pristine MWCNTs dispersed in aqueous solution showed an intense peak, λ_{max} 250 nm (data not shown)[40] but after the interaction with nafion this peak disappeared, indicating wrapping/interaction of nafion with MWCNTs. A peak observed with λ_{max} 300 nm in the UV–visible spectrum of free L was assigned to π- π^* transition of C=N present in L[41] and a broad hump observed at 400-500 nm was assigned to weak d–d-transition of ferrocene.[42] These peaks shifted to 310 nm and to 450-500 nm respectively in the spectrum of nanocomposite. It suggested that L was adsorbed on the surface of nafion coated MWCNTs. These spectral observations were also supported by the naked eye detection of colour change as depicted in inset to Fig.4. The blackish solution of MWCNTs/nafion [inset (1) to Fig. 4] changed to brown colour [inset (3) to Fig. 4] on addition of orange coloured solution of L [inset (2) to Fig. 4].

3.6 IR characterization of L/MWCNTs/nafion nanocomposite:

The adsorption of L on nafion coated MWCNTs surface was supported by IR spectra of L and L/MWCNTs/nafion nanocomposite. The IR spectrum of pure nafion reported earlier [33] showed peaks at 2500–3700 cm^{-1} which was diagnostic of water and sulfonic acid present in the nafion pores. The peak observed at 1634 cm^{-1} was assigned to -OH bending vibration whereas the peaks at 1452 cm^{-1} and 1057 cm^{-1} were assigned to C-F stretching and ether groups present in nafion. The IR spectrum of MWCNTs/nafion was observed as reported earlier.[26,33] The peak

observed at 1452 cm^{-1} is assigned to C-F stretching vibration which was shifted to 1432 cm^{-1}. It supported the interaction of hydrophobic per fluorocarbon chain to MWCNTs. The peak at 1634 cm^{-1} overlapped to the peak due to C=C of MWCNTs vibration. Upon addition of L on nafion coated MWCNTs (*cf.* Fig. 5), C-F stretching vibration was observed with a peak at 1464 cm^{-1}; C-S stretching frequency shifted from 992 cm^{-1} to 874 cm^{-1} and shifting of C=C stretching from 1634 to 1639 cm^{-1} probably due to overlap of C=C stretching vibration of MWCNTs with stretching vibration of C=N bonds present in L together with -OH bending vibration of nafion. Hence, it was inferred that L was adsorbed on nafion coated MWCNTs through noncovalent interaction.

3.7 Electrochemistry of L/MWCNTs/nafion nanocomposite modified electrode:-

CV was used to study the electrochemical properties of L/MWCNTs/nafion nanocomposite. Fig. 6 shows electrochemical behaviors of L/MWCNTs/nafion nanocomposite modified electrode at scan rates of 10-250 mV/s in 0.1M PBS (pH 7.1). In case of plain GCE and MWCNTs coated with nafion modified electrode, no redox peaks could be observed. CV was also performed for L/nafion composite but due to high leaching of L, CV was difficult to record as peak current keeps on decreasing continuously (data not shown). To discern the effect of substituent's attached to the ferrocene moiety which can alter the redox activity of ferrocene, we have also studied the electrochemistry of ferrocene-4-carboxyladehyde/MWCNTs/nafion (Fig. S5) and L/MWCNTs/nafion nanocomposite modified electrode (*cf.* Fig.6) and found that the CV of ferrocene-4-carboxyldehyde/MWCNTs/nafion modified electrode shows one peak due to ferrocene/ferrecenium ion (Fc/Fc^{+}) redox couple with the cathodic and anodic peak at 0.434 and 0.511 V respectively and an irreversible cathodic peak at 0.158 V. However, CV of L/MWCNTs/nafion nanocomposite modified electrode showed one redox peak of Fc/Fc^{+} redox couple (E_{pc}: 0.194 and E_{ac}: 0.372 V) along with a 'bump' or oxidative post peak (0.534 V). The two oxidative peaks in CV of L/MWCNTs/nafion modified GCE might be the result of the presence of both oxidation state of iron metal i.e. +2 and +3 when L were incorporated with MWCNTs/nafion. As discussed earlier, MWCNTs are solublized in nafion due to wrapping of hydrophobic part of nafion and sulphonic group protrudes out, making MWCNTs negatively charged which further help in the adsorption of L on MWCNTs/nafion via electrostatic interaction between Fe of metal. The peak current i_{pa}/i_{pc} was found to be less than 1 supporting

that L in its oxidized form is more stable in nafion film because of the increased positive charge. This also accounts for the poor reversibility of the redox process as evidenced by large peak separation of 178 mV at a scan rate 10 mV/s. Hence, the mechanism proposed is of successive electron transfer Fe^{II}– Fe^{II} → Fe^{II} – Fe^{III} and Fe^{II} – Fe^{III} → Fe^{III} – Fe^{III}.[43] The L/MWCNTs/nafion modified GCE exhibited high current density with the i_{pc} and i_{pa} of 29.0 x 10^{-6} and -18.8 x 10^{-6} A respectively in comparison to ferrocene-carboxyldehyde/MWCNTs/nafion modified GCE (i_{pc}; 0.43 x 10^{-6} i_{ac}; -2.0 x 10^{-6}A). On comparison to CVs of L/MWCNTs/nafion and ferrocene-4-carboxylic acid/MWCNTs/nafion, the redox couple of L was observed to shift towards cathodic direction which may be due to the effect of electron releasing moiety attached to L. The formal potential E^0 calculated from the midpoint between cathodic and anodic waves was found to be **0.283** V vs. Ag/AgCl reference electrode at scan rate of 10 mV/s. The effect of varying scan rates (υ) on peak current was investigated in the range of 10-250 mV/s. According to Randles-Sevicik plot [inset (I) to Fig. 6], it was found that anodic and cathodic peak currents increases linearly with scan rate. It showed that electrochemical reaction at L/MWCNTs/nafion nanocomposite modified GCE is a surface confined process. Furthermore, the voltammetric behaviour also indicates that nanocomposite has been immobilized on the surface of GCE.[44] The surface coverage area (AΓ) for the electroactive species was estimated using Eq. AΓ = Q/nF[44], where Q is the charge obtained by integrating the anodic peak at low scan rate (10 mV/s), n is the number of electrons involved per ferrocene molecules (n=1) and A (cm^2) is the geometric electrode area. In the present case, the value of AΓ was determined to be 6.7 x 10^{-8} mol cm^{-2}. Inset (II) to Fig. 6 shows the magnitudes of the peak potentials as a function of the logarithm of the potential scan rates. There is a linear dependence of E_p on log υ only at high scan rates. Kinetic parameters α (electron transfer coefficient) and k_s (standard rate transfer constant) were determined as indicated earlier. [45]A value of 0.42 for α and 0.017 M^{-1} s^{-1} for k_s was obtained. Therefore, it was concluded that L could easily be incorporated in MWCNTs/nafion complex from solution. Further, nafion acts as an effective ion exchanger for metal based complexes; and in presence of MWCNTs along with hydrazone there is an increase in the charge transfer which is relatively low in the pure nafion film.[45]

3.8 Electro-oxidation of azide on L/MWCNTs/nafion nanocomposite modified electrode:

The oxidation of azide was studied with both CV and DPV. To investigate the effect of substituent attached to ferrocene-4-carboxyldehyde to prepare L on the oxidation of azide, we have studied the azide oxidation on glutaric acid/MWCNTs/nafion, ferrocene-4-carboxyldehyde/MWCNTs/nafion and L/MWCNTs/nafion modified GCE. Fig. 7 shows the CVs of glutaric acid/MWCNTs/nafion, ferrocene-4-carboxyldehyde/MWCNTs/nafion and L/MWCNTs/nafion nanocomposite modified GCE in PBS (pH 7.1) in absence (curve a, c and e) and presence (curve b, d and f) of 2 mM aqueous solution of azide ion respectively. On addition of azide ion, the anodic peak current was enhanced 10 fold on L/MWCNTs/nafion (curve f, i_{ac}; 58.68 x 10^{-6} A) in comparison to ferrocene-4-carboxyldehyde/MWCNTs/nafion modified GCE (curve d, i_{ac}; 5.87 x 10^{-6} A) while no obvious change was observed on the addition of azide ion to MWCNTs/nafion modified GCE (Fig. 7 inset II) and glutaric acid/MWCNTs/nafion modified GCE (curve b, 2.8 x 10^{-6} A), indicating that L /MWCNTs/nafion facilitate the oxidation of azide. Electrocatalytic oxidation of azide occurred at more than 1V on bare GCE but on modification of electrode by L/MWCNTs/nafion nanocomposite, the oxidation of azide started at 0.30 V and reached maxima at 0.90 V. Nitrogen gas and various nitrogen oxides are formed during azide oxidation at platinum and gold electrodes,[15] while nitrogen gas was the only oxidation product formed at GCE due to relatively lower surface oxide coverage on glassy carbon than on metals.[1] In this study, the following mechanism is proposed for azide sensing: (1) Binding of azide to the acidic –NH moiety present in L (2) further the transfer of electron density to ferrocenyl center and consequently the Fc moiety get more easily oxidized to Fc^+ ion[46](Scheme 2). The selective binding of azide to the L might be due to the oxidation of Fc in the vicinity of the amide group, increases the acidity of the amide proton, making hydrogen-bonding stronger, and thus there is a synergy between ion-paring and H-bonding interactions. [47] Hence, it is proposed that in the first step, azide ion binds to Fc^+ cation which helps in the oxidation of azide and takes part in more sensitive determination of azide than other electrode system.

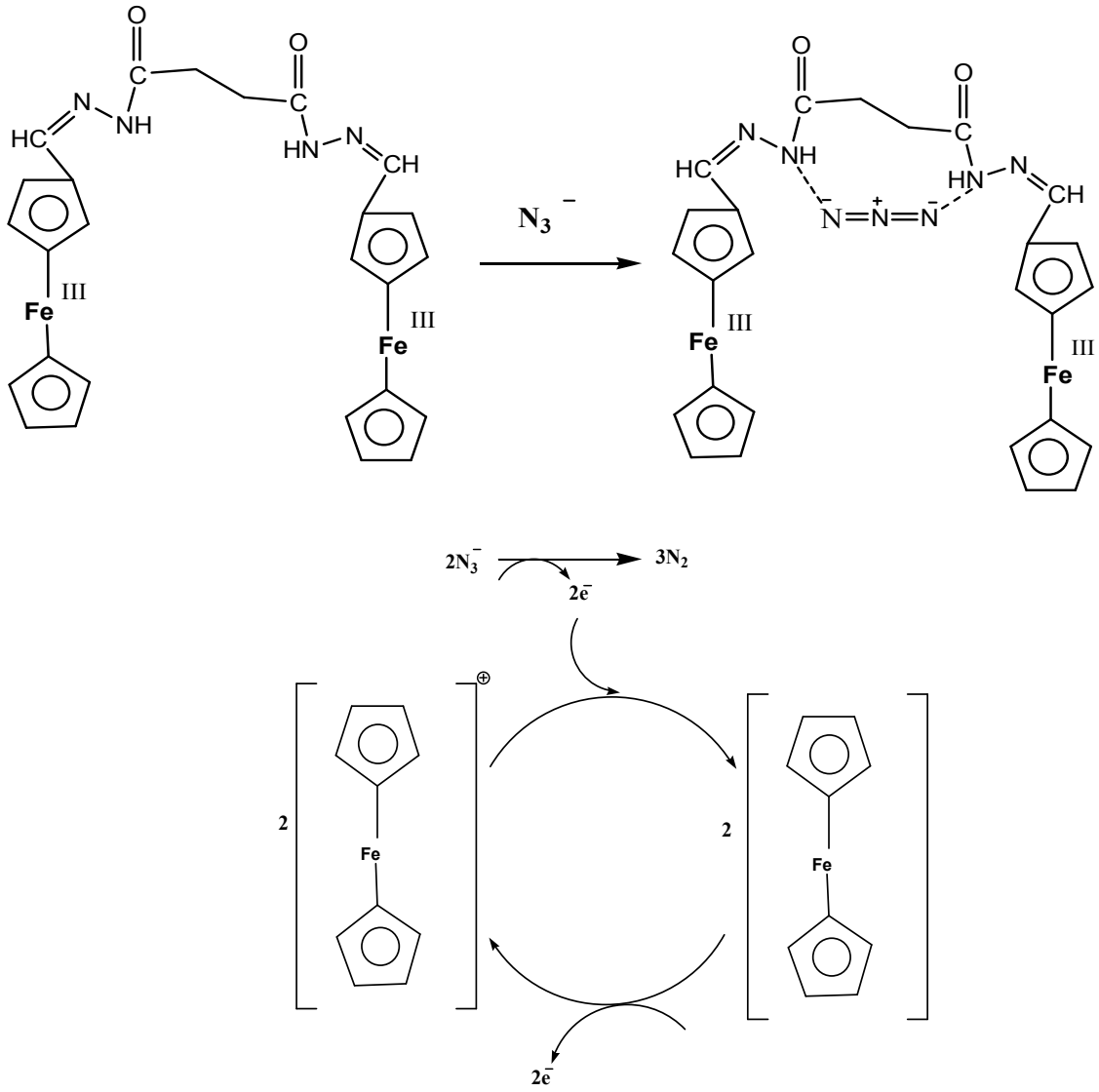

Scheme 2: Probable mechanism of azide oxidation on L/MWCNTs/nafion modified GCE

Fig. 8 shows DPV response on L/MWCNTs/nafion nanocomposite modified electrode after addition of increasing concentrations of azide ion. It could be inferred that presence of MWCNTs enhanced the electron transportation between electrode and analyte. Further, the voltammetric results indicated that L and MWCNTs could synergistically catalyze the electrochemical oxidation of azide ions.

4. Optimization of experimental conditions:

4.1. *Effect of varying composition*

The composition of substance used for electrode modification causes change in the modified electrode properties. Hence for studying this effect, we have optimized the ratio of different components such as nafion, MWCNTs and L used for modification of GCE. Nafion and MWCNTs have been taken in different ratios for preparing nanocomposite as indicated in table 2. The results obtained for the oxidation of 0.0422 mM azide at subsequent electrodes [Fig. S7(A) for nafion, (B) for MWCNTs, (C) for L] indicates that the optimized ratio used for the preparation of L/MWCNTs/nafion nanocomposite in the present work is most suitable for effective working of the electrode.

4.2. Effect of deposition time:

We have optimized the deposition time for improved signals. The effect was monitored by studying the performance of electrode with the help of CV technique (Fig. S7 (D)) which shows the electrode performance increases on increasing the deposition time but beyond 1 hour the electrode becomes stable.

4.3. Effect of pH:

We have also studied the effect of pH on the performance of modified electrode by CV under similar conditions with PBS of different pH and found that the maximum current was observed at pH 7.1 but no change in potential was observed. Hence, pH 7.1 was used as optimized pH for performing the experiment (Fig. S7 (E)).

5. Performance of L/MWCNTs/nafion nanocomposite modified electrode**:**

5.1 Selectivity against interferences:

Interference studies were performed to evaluate the selectivity of the sensor in presence of various anions such as cyanide, nitrate, nitrite, fluoride, chloride, bromide, iodide, hydrogen

sulphate, dihydrogen phosphate and acetate which can act as interfering substances. It was found that the tested substances did not interfere with the determination of azide ion at 1.86 mM. The current obtained for each interfering substance (ten times concentrated than azide solution) through CV studies was negligible when compared with the current obtained in the presence of azide (Fig. S6). For the detection of azide in real samples, synthetic samples were prepared by adding known amounts of azide in the tap water and the concentration of azide spiked tap water was studied by using standard addition method. In this work excellent recovery was obtained by adding 45 µM azide spiked tap water sample on L/MWCNTs/nafion modified GCE and 43.8 (±0. 30) µM (n=4) azide was recovered (-2.6 % recovery). The validation of real sample was also performed using spectrophotometric determination for the same concentration of azide (45 µM) and 45.8 (±0.30) µM (n=4) of azide was recovered (1.76 % recovery). This data shows results are in good agreement with the standard measurement indicating that proposed sensor can be applied successfully for the determination of azide.

5.2. Calibration plot:

Inset to Fig. 8 shows the calibration plot for prepared sensor using DPV method. A linear calibration equation was observed as $I_p = 0.3167\ C\ [mM] + 0.4450$ ($R^2 = 0.9926$, n= 12) ranging from 0.020 mM to 20 mM of azide ion in 0.1M phosphate buffer solution at pH 7.1. The detection limit was calculated using formula $DOL = k\ S_b/S$, where, S is sensitivity of the method (determined as slope of the calibration curve), S_b is the standard deviation of the blank measurement, k is the statistical constant (a value of k=3 is strongly recommended by IUPAC, based on the confidence interval).[29] The detection limit was calculated as 0.312 µM. The responses are at par/better as compared to other reported works indicating the suitability of the prepared nanocomposite material (table 3).

5.3. Robustness studies of L/MWCNTs/nafion nanocomposite modified GCE:

The stability of the electrode was studied electrochemically. There was no appreciable change in the peak current of L/MWCNTs/nafion nanocomposite modified GCE after 20 repeated cycles as shown in Fig.9, justifying the stability of L incorporated in nafion film along with MWCNTs. As discussed above (Fig. 4), the CV of L/MWCNTs/nafion modified GCE shows a redox peak due to Fc/Fc^+ along with the oxidative post peak which was found to disappear as shown in Fig.

9. The probable reason behind this might be exposer of electrodes for longer periods of time in the bulk solution.[53]

When 20 continuous cycles scan was carried out at 10 mV/s scan rate, only 6.8% decrease of the initial response at 1.86 mM azide was recorded. The RSD of 1.5% was observed for three successive measurements of one nanocomposite modified electrode at 1.86 mM azide indicating good reproducibility of the proposed sensor. The long term stability of proposed sensor was also studied. Lifetime was found more than 4 months when the electrode was kept at ambient conditions. The response of azide was tested intermittently. During the first 3 days, the response current shows about 5% decrease.

5. Conclusion:

A new ferrocenoyl glutaric acid hydrazone (L) is prepared and characterized followed by the preparation of a nanocomposite material consisting of L/MWCNTs/nafion. The latter is fabricated as an amperometric azide sensor without any interference with other anions. The interaction of nafion polymer with MWCNTs provides sulphonic groups functionalized MWCNTs which can interact with L via electrostatic interaction and gives L/MWCNTs/nafion nanocomposite without changing the native structure of prepared hydrazone (L) and the structure properties of MWCNTs.

Acknowledgements:

Authors are grateful to authorities of DRDO and DBT, New Delhi, India projects sanction No. ERIP/ER/1003880/M/01/1391 and BT/PR1791/MED/32/174/2011 respectively for the financial assistance. We are also thankful to Mrs. Madhu Yashpal (Scientist, Electron Microscopy Facility, IMS, BHU) for TEM analysis.

References:

1. J. Xu and G.M. Swain, *Anal. Chem*., 1998, **70**, 1502–1510.
2. S. Chang and S. H. Lamm, *Int. J. Toxicol.*, 2003, **22**, 175–186.
3. H. D. Fair and R. F. Walker, in Energetic materials. Plenum, New York, 1997, Page 501.
4. B. D. Pollock, W. J. Fisco, H. Kramer and A. C. Forsyth, in Energetic materials-2, Plenum, New York, 1977, Ch.3, Pages 73-159.

5. P. I. Anable and L. A. Sly, *J. Chromatogr*, 1991, **546**, 325–334.
6. S. Kage, K. Kudo and N. Ikeda, *J. Anal. Toxicol*., 2000, **24**, 429–432.
7. T. Schroder, M. Gartner, T. Graba and S. Brase, *Org. Biomol. Chem.*, 2007, **5**, 2767–2769.
8. F. Daigle, F. Trudeau, G. Robinson, M. R. Smyth and D. Leech, *Biosens. Bioelectron*., 1998, **13**, 417–425.
9. K. Tsuge, M. Kataoka andY. Seto, *J. Anal. Toxicol.*, 2001, **25**, 228–236.
10. R. Prasad, V. K. Gupta andA. Kumar, *Anal. Chim. Acta*., 2004, **508**, 61–70.
11. A. K. Singh, U. P. Singh, V. Aggarwal and S. Mehtab, *Anal. Bioanal. Chem.*, 2008, **391**, 2299–2380.
12. M. Ghaedi, M. Montazerozohori and R. Sahraei, *J. Indust. Eng. Chem.,* 2013, **19**, 1356–1364.
13. M. Ghaedi, S. Naderi, M. Montazerozohori, R. Sahraei, A. Daneshfar and N. Taghavimoghadam, *Mater. Sci. Eng. C*, 2012, **32**, 2274–2279.
14. M. Ghaedi, M. Pakniat, Z. Mahmoudi, S. Hajati, R. Sahraei andA. Daneshfar, Spectrochim. Acta Part A: Mol. Biomol. Spect., 2014, **123,** 402–409.
15. A. Dalmia, S. Wasmus, R. F. Savinell and C. C. Liu, *J. Electrochem. Soc.*, 1996, **143**, 556–560.
16. P. Stepnicka, Ferrocenes: Ligands, Materials and Biomolecules, Wiley, Chichester, Eds. 2008.
17. M. Fuentealba, Z. J. Hamon, D. Carrilloa and C. Manzur, *New J. Chem.*, 2007, **31**, 1815–1825.
18. J. A. Thomas, *Dalton Trans.*, 2011, **40**, 12005-12016.
19. B. Rout, L. Unger, G. Armony, M. A. Iron and D. Margulies, *Angew. Chem. Int. Ed.*, 2012, **51**, 12477–12481.
20. K. Kavallieratos, S. Hwang and R. H. Crabtree, *Inorg. Chem.* 1999, **38**, 5184-5186.
21. M. Mazur and G.J. Blanchard, *J. Phys. Chem. B*, 2005, **109**, 4076-4083.
22. M. Liebau, H.M. Janssen, K. Inoue, S. Shinkai, J. Huskens, R.P. Sijbesma, E.W. Meijer and D.N. Reinhoudt, *Langmuir*, 2002, **18**, 674-682.
23. A. T. A. Jenkins and J. F. L. Meur, *Electrochem. Commun*., 2004, **6**, 373-377.
24. J. Razumienė, V. Gurevičienė, A. Vilkanauskytė, L. Marcinkevičienė, I. Bachmatova, R. Meškys and V. Laurinavičius, *Sens. Actuators B*, 2003, **95**, 378-383.
25. V. S. Tripathi, V. B. Kandimalla and H. X. Ju, *Biosens. Bioelectron.*, 2006, **21,** 1529-1535.
26. I. Tiwari, M. Gupta, P. Sinha andS.K. Aggarwal, *Electrochimica Acta,* 2012, **76**, 106–111.
27. I. Tiwari, M. Gupta, P. Sinha and C. E. Banks, *Mat. Res. Bull.,* 2014, **60**, 166–173.
28. I. Tiwari, K. P. Singh, B.C. Upadhyay and V. S. Tripathi, *Anal. Lett.*, 2010, **43**, 2019-2030.
29. I. Tiwari and M. Singh, *Microchim. Acta* . 2011, **174**, 223-230.

30. I. Tiwari, K. P. Singh and M. Singh, *Russ. J. Gen. Chem.*, 2009, **12**, 2685-2694.
31. I. Tiwari, K.P. Singh and C.E. Banks, *Anal. Meth.*, 2012, **4**, 118-124.
32. M. Ghaedi, M. Montazerozohori, S. Khodadoust and M. Behfar, IEEE Sensors Journal, 2013, **13,** 321-327.
33. E. Hwang, I. A. Levitsky and W. B. Euler, *J. Appl. Polym. Sci.,* 2010, **116**, 2425-2432.
34. A. N. Chakoli, J. He, W. Cheng andY. Huang, *RSC Adv.*, 2014, **4**, 52372-52378.
35. M. M. Khan**,** V. Filiz**,** G. Bengtson**,** S. Shishatskiy**,** M. Rahman **and**V. Abetz, *Nanoscale Res Lett.,* 2012, **7**:504.
36. F. J. F. Carretero, V. Compan and E. Riande, *J. Power Sources*, 2007, **173**, 68-76.
37. H. S. Park, Y. J. Kim, W. H. Hong, Y. S. Choi and H. K. Lee, *Macromolecules*., 2005, **38**, 2289-2295.
38. J. Lu, S. Lu and S.P. Jiang, *Chem. Commun.***,** 2011, **47**, 3216-3218.
39. L. Liu, Y. H. Su, C. M. C. Suryani, D. M. Wang and J. Y. Lai, *J. Mater. Chem*., 2010, **20**, 4409–4416.
40. Y. Liu, J. Lei and H. Ju, *Talanta*, 2008, **74,** 965–970.
41. J. Sørensen and M. F. Nielsen*, Cent. Eur. J. Chem.*, 2011, **9**, 610-618.
42. Z. Liang, W. Chena, J. Liu, S. Wang, Z. Zhoua, W. Li, G. Suna and Q. Xin , *J. Membr. Sci.*, 2004, **233**, 39–44.
43. J. E. Bercaw,A. C. Durrell, H.B. Gray,J.C. Green,N.Hazari,J.A. Labinger and R. Winkler, *Inorg.Chem*. 2010, **49**, 1801–1810
44. A J. Bard and L. R. Faulkner, Electrochemical Methods, Fundamentals and Applications, John Wiley Sons., Second ed., New York, 2001.
45. E. Laviron, *J. Electronal. Chem.,* 1979, **101**, 19-28.
46. Q. Y. Cao, T. Pradhan, S. Kim and J. S. Kim, *Organic Lett.*, 2011, **13**, 4386–4389.
47. C. Valerio, J. L. Fillaut, C. Valero, J. Ruiz, J. Guitlard, D. Austruc, *J. Am. Chem. Soc.*, 1997, 119, 2588-2589.
48. D. Leech and F. Daigl, *Analyst.*, 1998, **123**, 1971–1974.
49. V. Christova-Bagdassarian and M. Atanassova, *J. University Chem. Tech Metall.,* 2007, **42**, 311-314
50. M. Ghaedi, A. Shokrollahi, M. Montazerozohori and S. Derk, *IEEE Sensors Journal.*, 2010, **10**, 814-819.
51. A.K. Singh, U.P. Singh, V. Aggarwal and S. Mehtab. *Anal Bioanal Chem,* 2008 **391**, 2299–2308.
52. R. Prasad, V.K. Gupta and A. Kumar, *Anal. Chim. Acta*, 2004, **508**, 61–70.
53. S. Zhang, W. Yang, Y. Niu and C. Sun, *Sens. Actuat. B,* 2004, **101**, 387-393.

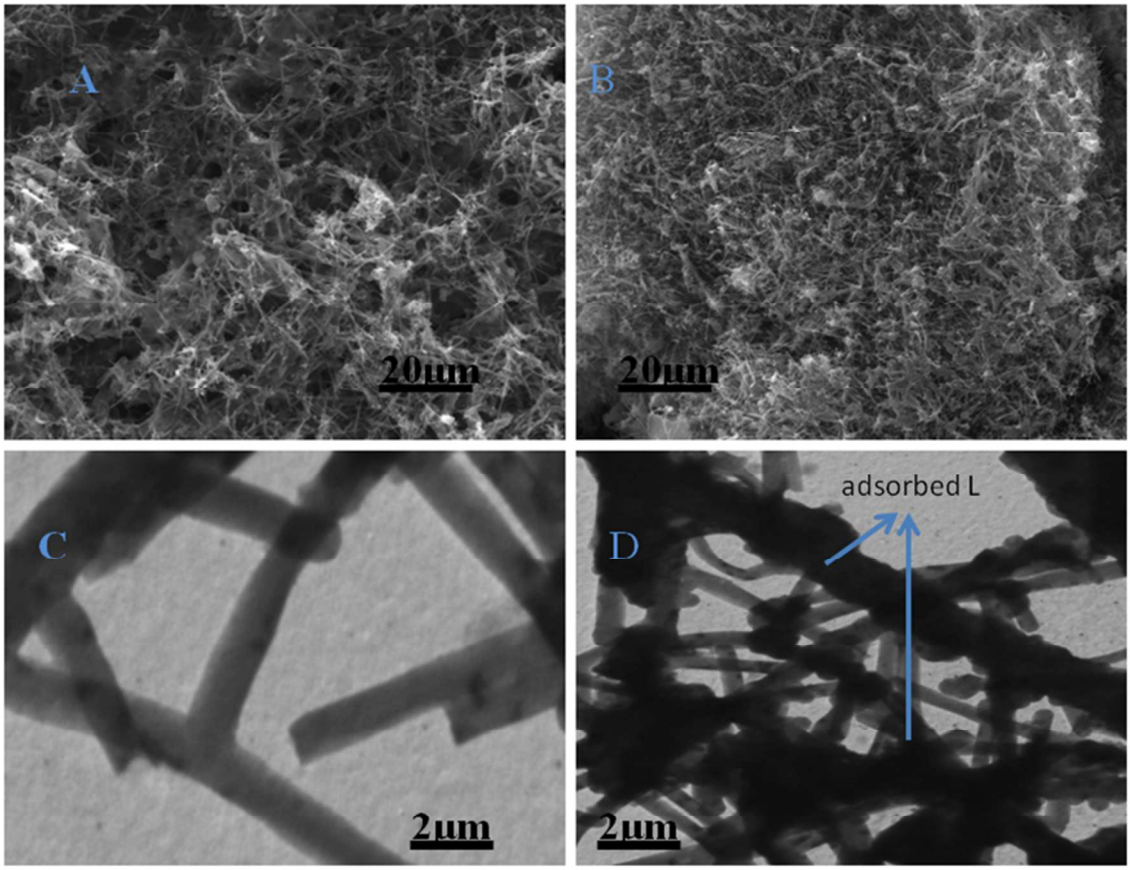

Fig.1(a) SEM image of MWCNTs/Nafion, (b) SEM image of L/MWCNTs/nafion nanocomposite, (c) TEM image of MWCNTs/nafion and (d) TEM image of L/MWCNTs/nafion nanocomposite.

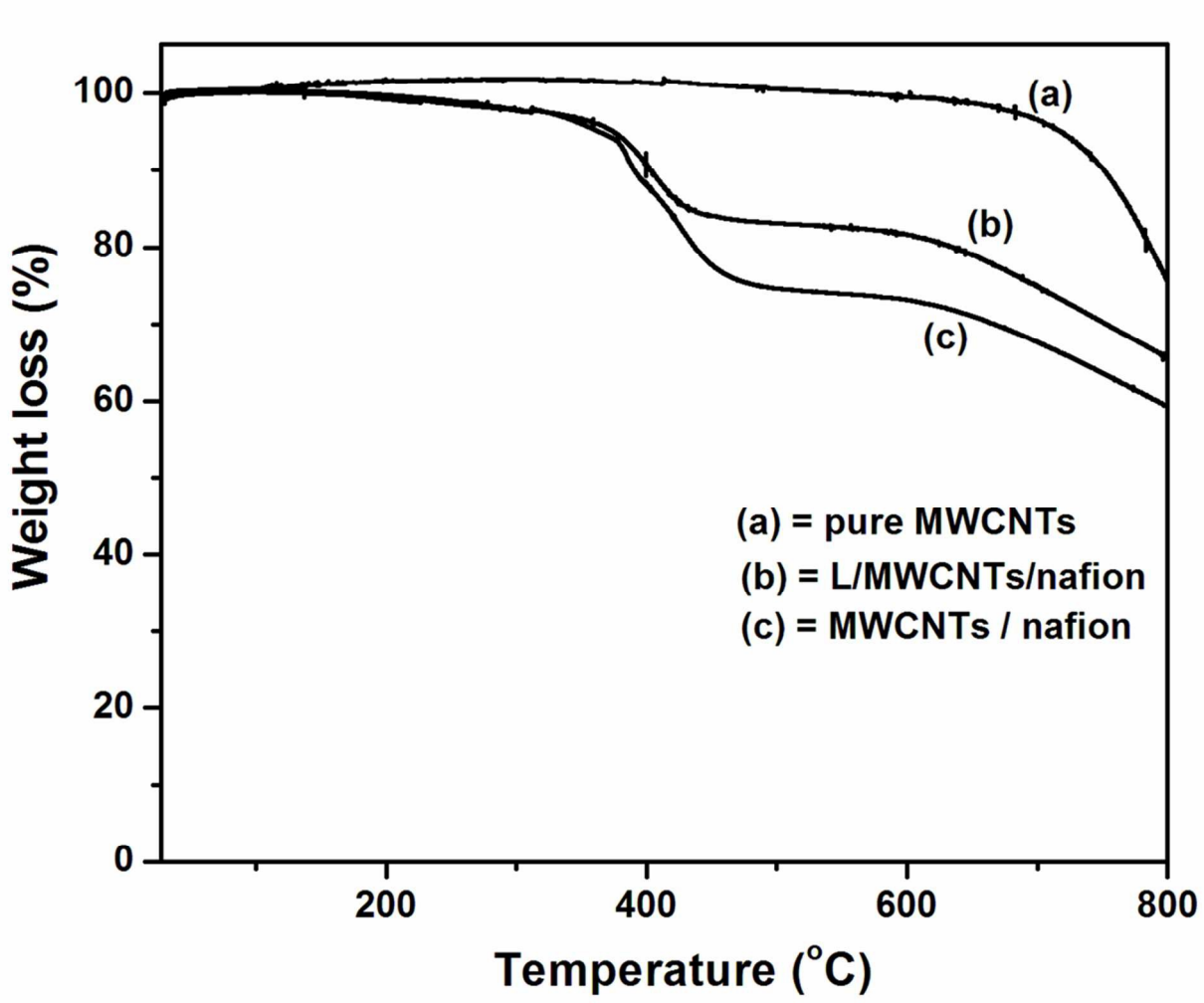

Fig. 2 Thermogravimetric analysis scans of (a) pure MWCNTs (b) L/MWCNTs/nafion (c) MWCNTs/nafion under air atmosphere and heating rate 10 ^{0}C min^{-1} from room temperature to 800 ^{0} C.

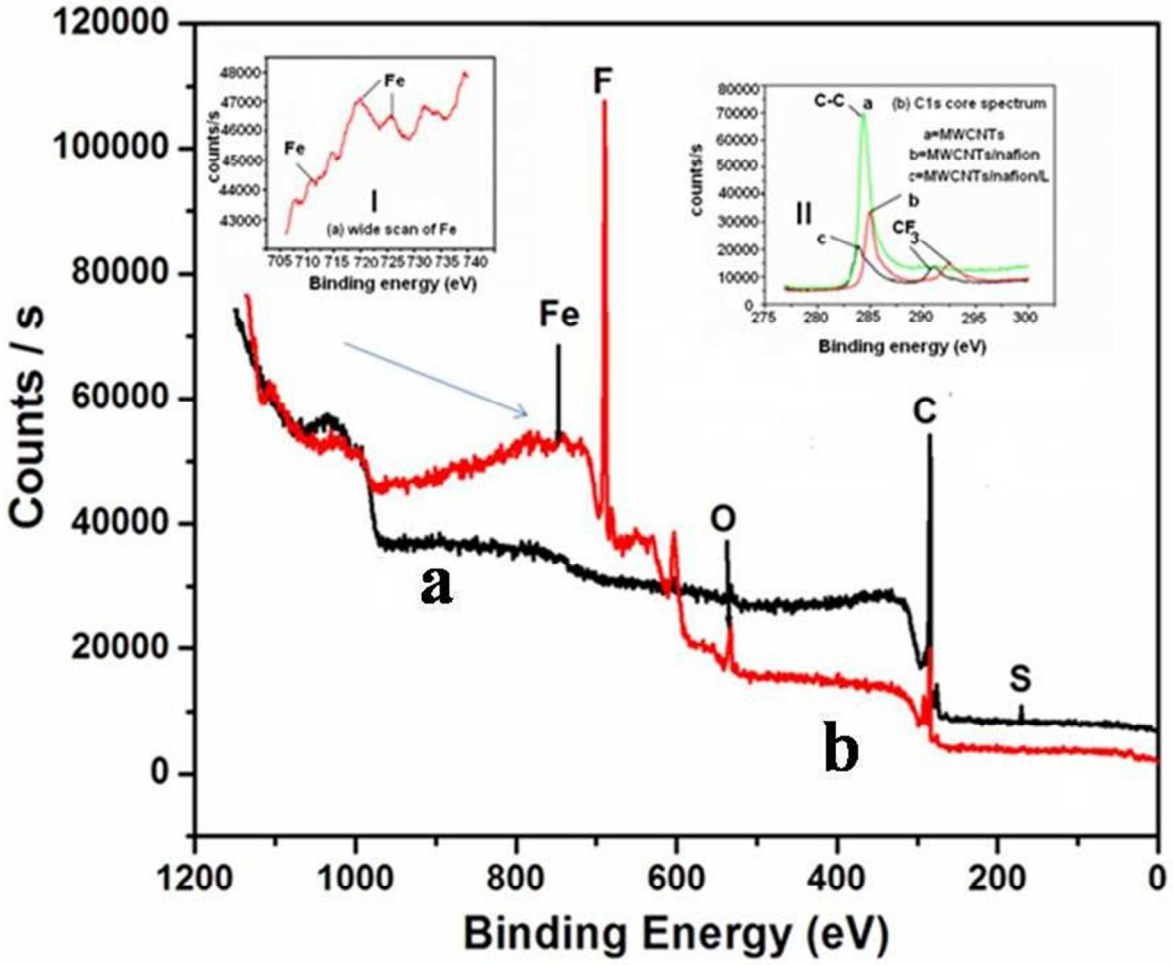

Fig.3 XPS comparison of pure MWCNTs (curve a) and L/MWCNTs/nafion (curve b). Inset I. (I) Wide scan of Fe in L/MWCNTs/nafion showing enlargement of iron peak; Inset II.(II) C1s Core spectrum of carbon of (a) pure MWCNTs, (b) MWCNTs/nafion and (c) L/MWCNTs/nafion nanocomposite.

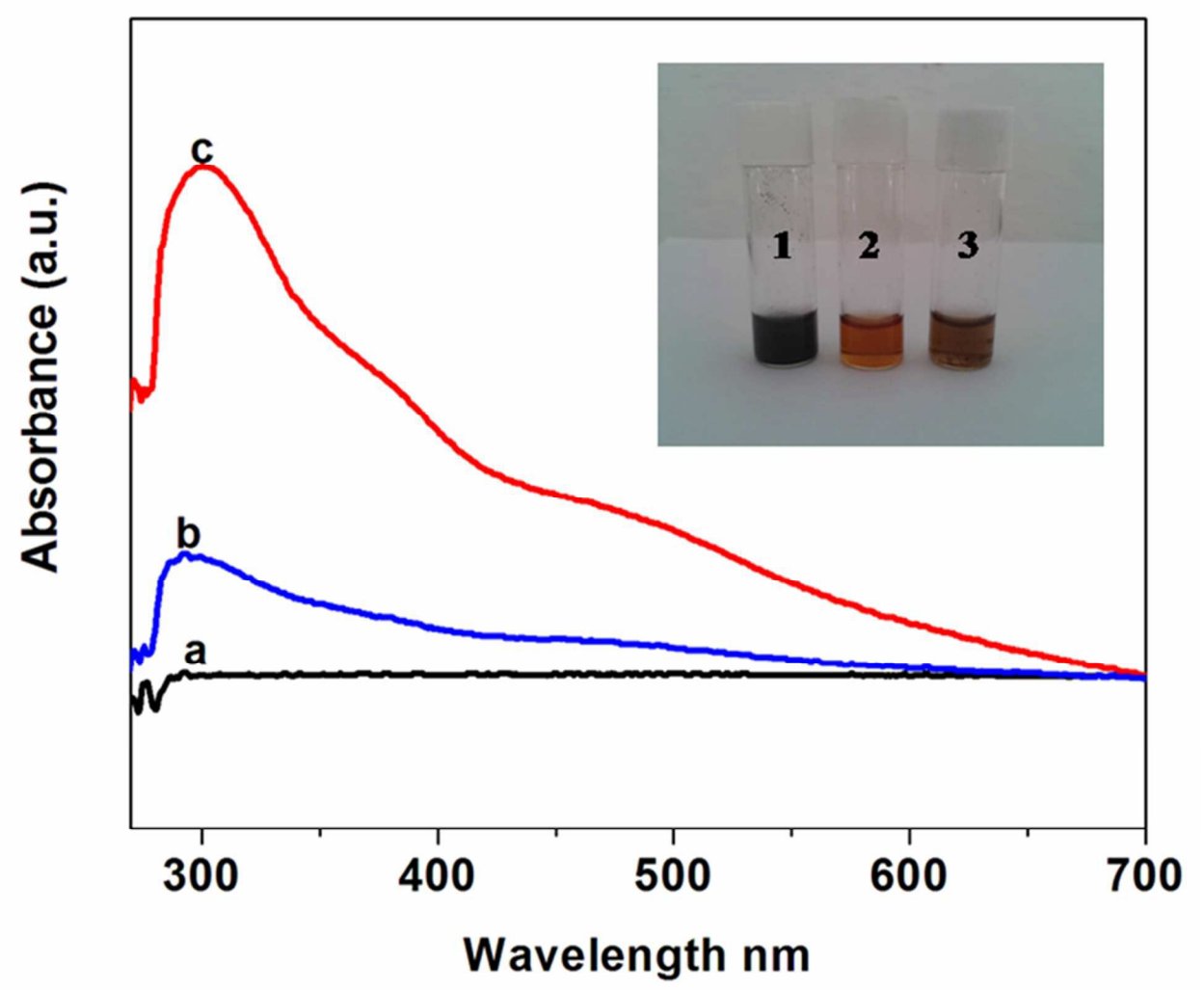

Fig.4 UV-Vis of (a) MWCNTs/nafion, (b) L aqueous solution and (c) L/MWCNTs/nafion nanocomposite; Inset (1) Photograph of MWCNTs/nafion, Inset (2) Photograph of L aqueous solution, Inset (3) Photograph of L/MWCNTs/nafion nanocomposite.

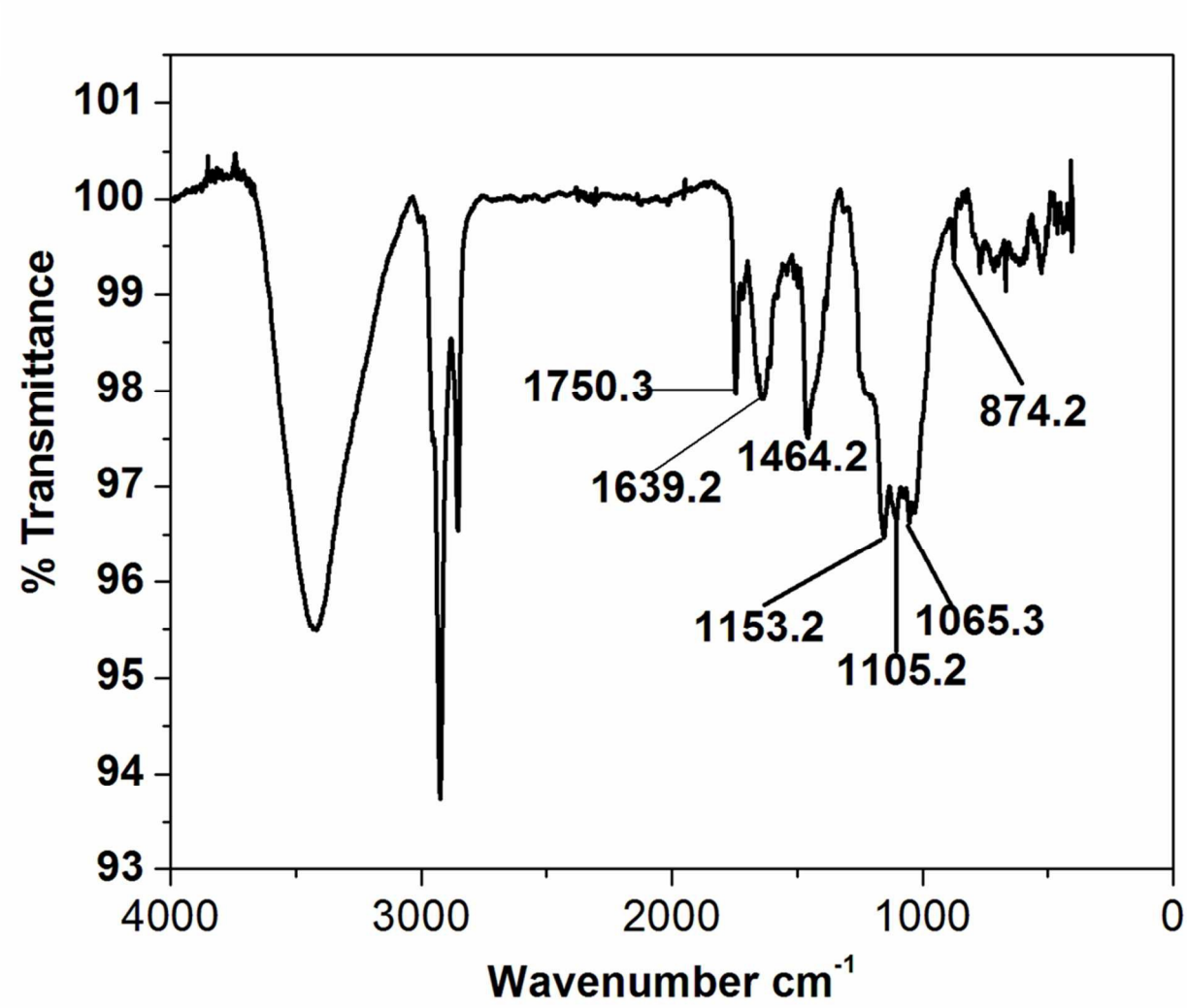

Fig.5 FTIR spectra of L/MWCNTs/nafion nanocomposite.

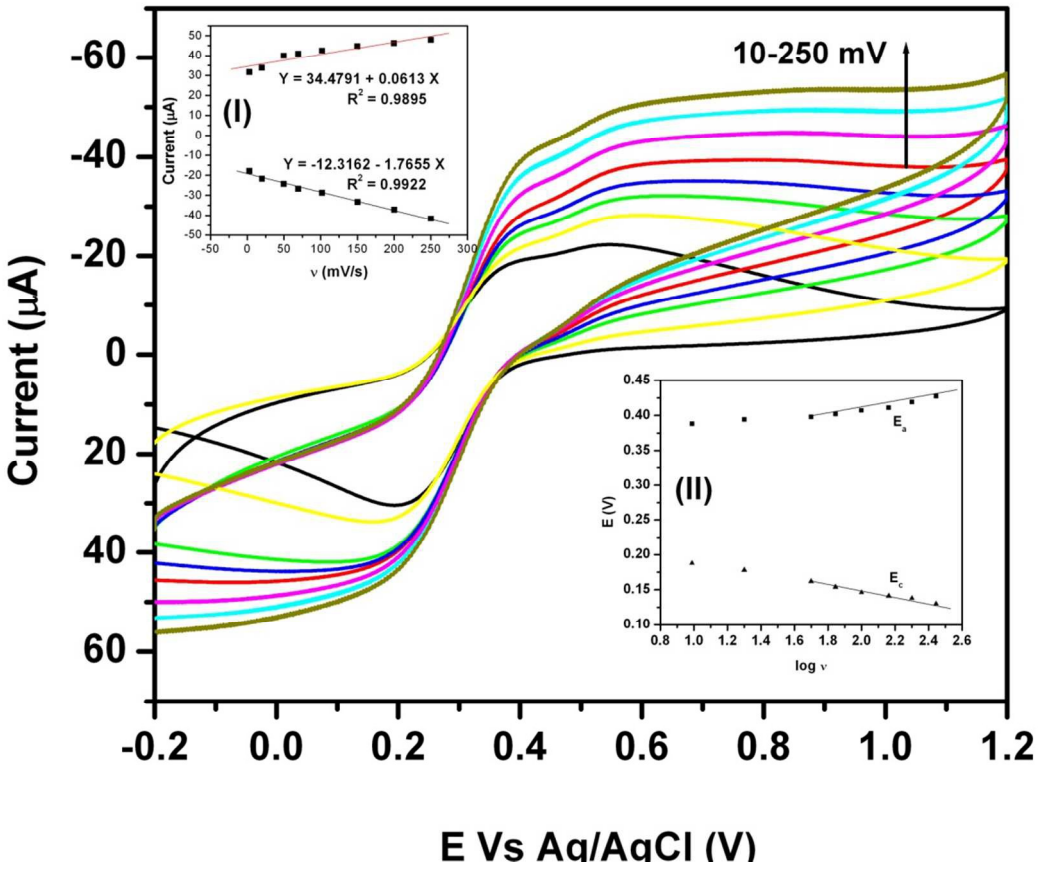

Fig.6 CV of L/MWCNTs/nafion nanocomposite modified electrode at different scan rates 10, 20, 50, 70, 100, 150, 200, 250 mV s^{-1}. Inset I: Randles-Sevcik plot; Inset II: Plot of peak potentials as a function of logarithm of the potential scan rates.

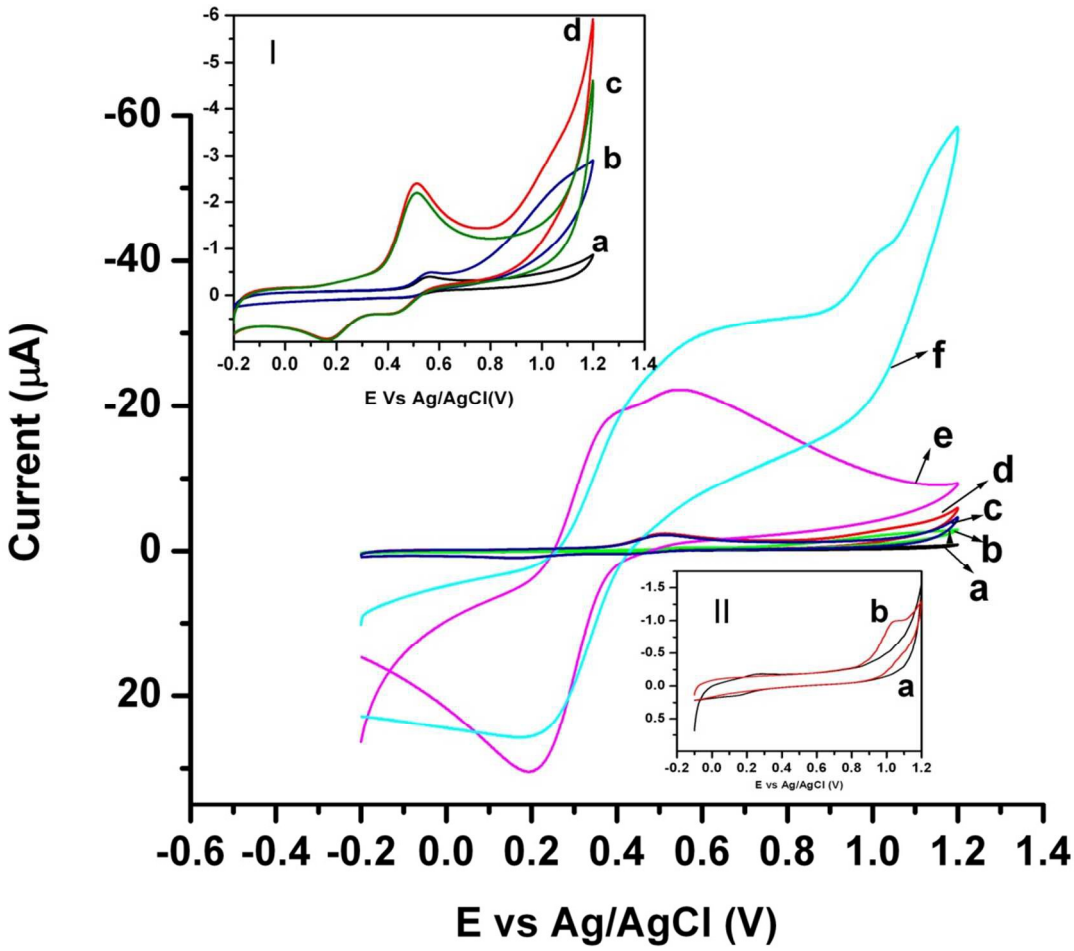

Fig.7 CVs of glutaric acid/MWCNTs/nafion, ferrocene-4-carboxyldehyde/MWCNTs/nafion and L/MWCNTs/nafion nanocomposite modified GCE in PBS (pH 7.1) in absence (curve a, c and e) and presence (curve b,d and f) of 2 mM aqueous solution of azide ion respectively. Inset (I): Enlarged images of a,b,c, and d. Inset (II): CV of MWCNTs/nafion modified GCE in the absence (curve a) and presence of 2 mM aqueous solution of azide ion (curve b).

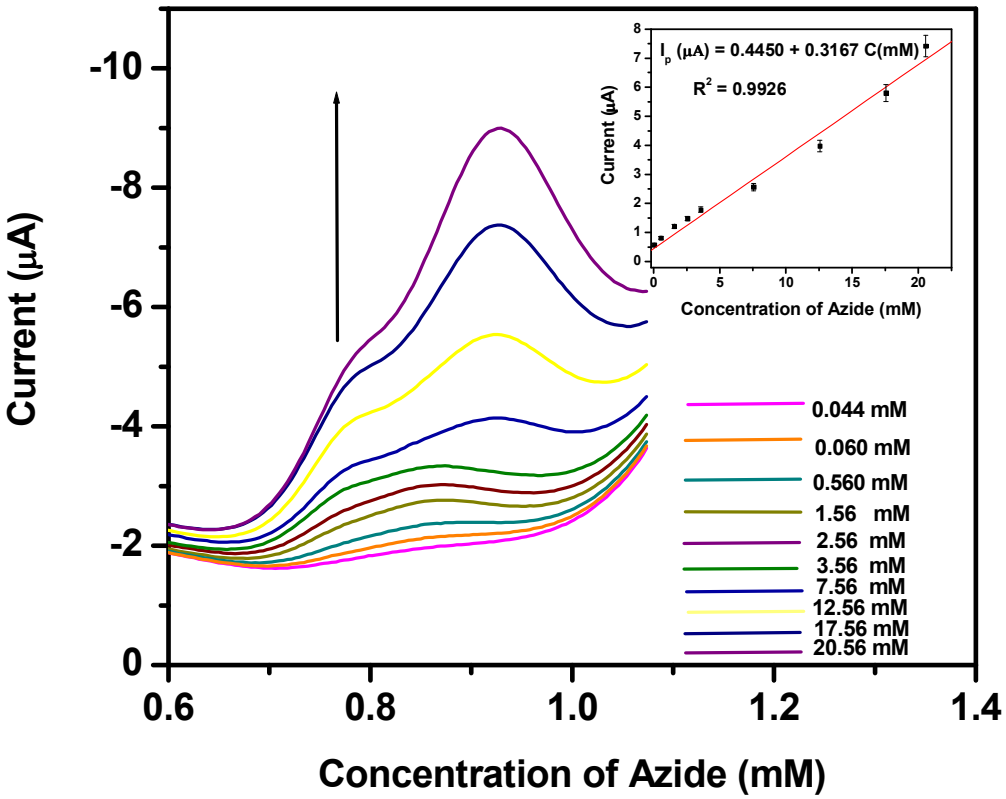

Fig.8 DPV response of different concentration of azide, inset to Fig.8 Calibration plot with error bar.

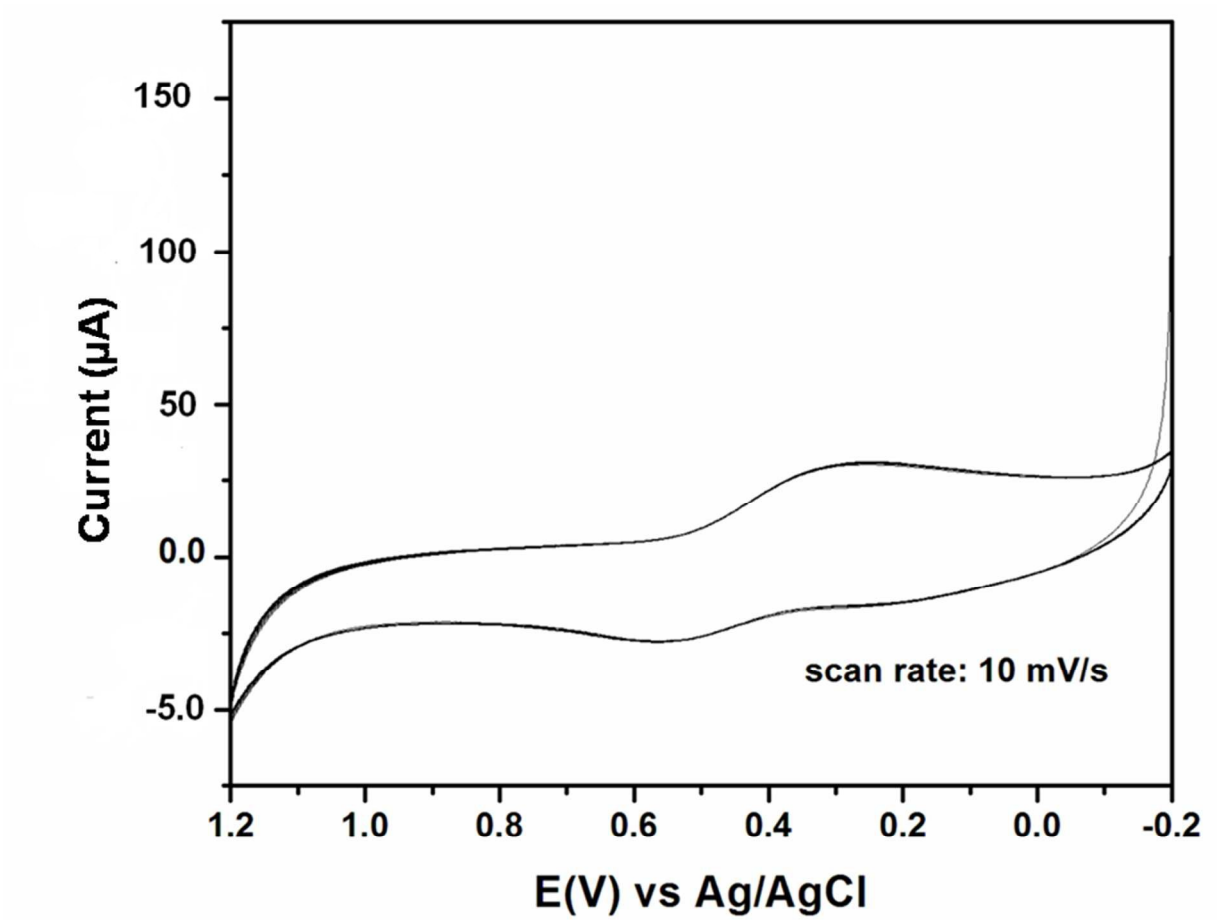

Fig.9 Cyclic Voltammetry of 20 repeated cycle of L/MWCNTs/nafion nanocomposite modified electrode at 10 mV/s scan rate in pH 7.1 PBS.

IR (KBr): ν_{max}/cm^{-1}	^1H NMR (DMSO-d_6, δ ppm)	ESI-Mass spectroscopic data
3060, 3030 (NH) 1640 (C=O), 1601(CH=N), 812(cp), ,820, 635,507, 482 (Fe-cp).	11.0 (s, 1H; NH), 10.9 (s, 1H; NH), 7.98 (s, 1H; CH=N) , 7.78 (s, 1H; CH=N), 4.82-4.19 (m, 16H; Fc), 2.5(s, 2H; CH_2), 2.2(s, 2H; CH_2), 1.8(s, 2H; CH_2)	mass (*m*/*z*); 553.12 $[M+H]^+$, calcd. mass 552 ($C_{27}H_{28}N_4O_2Fe_2$).

Table 1: Spectroscopic Characterization of ferrocenoyl glutaric acid hydrazone.

Table 2. Preparation of nanocomposite using Nafion, L and MWCNTs taken in different ratios.

System A	MWCNTs (mg)	nafion (wt %,100 µL)	L (0.01 M)	Ratio of MWCNT and nafion
1	0.5	2	5 µL	1:4
2	0.5	1.6	5 µL	1:3.2
3	0.5	1.1	5 µL	1:2.2
4	0.5	0.8	5 µL	1:1.6
5	0.5	0.5	5 µL	1:1
B				
1	0.5	1.1	5 µL	1:4
2	1	1.1	5 µL	1:3.2
3	1.5	1.1	5 µL	1:2.2
4	2	1.1	5 µL	1:1.6
C				
1	0.5	1.1	5 µL	1:2.2
2	0.5	1.1	10 µL	1:2.2
3	0.5	1.1	15 µL	1:2.2
4	0.5	1.1	20 µL	1:2.2

Table 3: Comparison of linear range and detection limit of some modified electrode and L/MWCNTs/nafion modified GCE for the oxidation of Azide

Serial no.	Type of sensor construction	Technique	Linear range (M)	Detection limits	References
1.	GC-MS	extractive alkylation	1.0 x10^{-9} to 2 x10^{-7}	0.5 x10^{-9}	[6]
2.	Spectrometric determination of Ferric azide at 450nm	Microdiffusion	0 to 7 x 10^{-3}	0.5 x10^{-3}	[9]
3.	Reagentless laccase electrode	Amperometry	-	2.5 x10^{-6}	[48]
4.	Determination of sodium Azide at 450nm	Spectrometric	1.54 x 10^{-4} to 1.54 x10^{-2}	1.2 x 10^{-4}	[49]
5.	Schiff's base complex of Fe(III)/carbon paste electrode	Potentiometry	1.0 x 10^{-6} to 5.0 x10^{-2}	8.8 x 10^{-7}	[50]
6.	iron(III) hydrotris (3,5-dimethylpyrazolyl)borate acetylacetonate chloride [TpMe2Fe(acac)Cl] as a neutral carrier for an azide-selective electrode	Potentiometry	6.3 x10^{-7} to 1x 10^{-2}	3.8 x 10^{-7}	[51]
7.	iron(III) and Co(III) Complex (OBTAP)	Potentiometry	8.9 x10^{-5} to 10.0	1.0 x10^{-6}	[52]
8.	L/MWCNTs/ nafion GCE	Differential pulse voltammetry	2.0 x 10^{-5} to 2 x 10^{-2}	0. 312 x 10^{-6}	Present work